Title

Downregulation of the CpSRP43 gene expression confers a truncated light-harvesting antenna (TLA) and enhances biomass and leaf-to-stem ratio in Nicotiana tabacum canopies

Journal

Planta, 248(1)

ISSN

0032-0935

Authors

Kirst, Henning

Shen, Yanxin

Vamvaka, Evangelia

et al.

Publication Date

2018-07-01

DOI

10.1007/s00425-018-2889-7

Peer reviewed

Planta (2018) 248:139–154
https://doi.org/10.1007/s00425-018-2889-7

ORIGINAL ARTICLE

Downregulation of the *CpSRP43* gene expression confers a truncated light-harvesting antenna (TLA) and enhances biomass and leaf-to-stem ratio in *Nicotiana tabacum* canopies

Henning Kirst[1] · Yanxin Shen[2] · Evangelia Vamvaka[1] · Nico Betterle[1] · Dongmei Xu[2] · Ujwala Warek[2] · James A. Strickland[2] · Anastasios Melis[1]

Received: 8 January 2018 / Accepted: 29 March 2018 / Published online: 6 April 2018

Abstract

Main conclusion **Downregulation in the expression of the signal recognition particle 43 (*SRP43*) gene in tobacco conferred a truncated photosynthetic light-harvesting antenna (TLA property), and resulted in plants with a greater leaf-to-stem ratio, improved photosynthetic productivity and canopy biomass accumulation under high-density cultivation conditions.**

Evolution of sizable arrays of light-harvesting antennae in all photosynthetic systems confers a survival advantage for the organism in the wild, where sunlight is often the growth-limiting factor. In crop monocultures, however, this property is strongly counterproductive, when growth takes place under direct and excess sunlight. The large arrays of light-harvesting antennae in crop plants cause the surface of the canopies to over-absorb solar irradiance, far in excess of what is needed to saturate photosynthesis and forcing them to engage in wasteful dissipation of the excess energy. Evidence in this work showed that downregulation by RNA-interference approaches of the *Nicotiana tabacum signal recognition particle 43* (*SRP43*), a nuclear gene encoding a chloroplast-localized component of the photosynthetic light-harvesting assembly pathway, caused a decrease in the light-harvesting antenna size of the photosystems, a corresponding increase in the photosynthetic productivity of chlorophyll in the leaves, and improved tobacco plant canopy biomass accumulation under high-density cultivation conditions. Importantly, the resulting TLA transgenic plants had a substantially greater leaf-to-stem biomass ratio, compared to those of the wild type, grown under identical agronomic conditions. The results are discussed in terms of the potential benefit that could accrue to agriculture upon application of the TLA-technology to crop plants, entailing higher density planting with plants having a greater biomass and leaf-to-stem ratio, translating into greater crop yields per plant with canopies in a novel agronomic configuration.

Keywords Canopy density · Chlorophyll-deficient mutant · Light-harvesting antenna size · Productivity · TLA technology

Abbreviations

Car	Carotenoids
Chl	Chlorophyll
NPQ	Non-photochemical quenching
PS	Photosystem
TLA	Truncated light-harvesting antenna
TLA3-RNAi	*Nicotiana tabacum TLA3-CpSRP43* gene downregulation of expression by RNA interference

Electronic supplementary material The online version of this article (https://doi.org/10.1007/s00425-018-2889-7) contains supplementary material, which is available to authorized users.

✉ Anastasios Melis
melis@berkeley.edu

[1] Department of Plant and Microbial Biology, University of California, Berkeley, CA 94720-3102, USA

[2] Biotechnology Division, Altria Client Services, Richmond, VA 23219, USA

Introduction

Photosynthetic organisms, including bacteria, algae, and plants, have evolved extensive arrays of light-harvesting pigments, comprising chlorophylls (Chl), carotenoids (Car), and bilins that absorb sunlight and transfer the excitation energy

to photochemical reaction centers. The latter converts the absorbed irradiance to chemical energy via the photochemical charge separation reaction, which is viewed as the beginning step of photosynthesis. The evolution of sizable arrays of light-harvesting antennae in all photosynthetic systems confers a selective survival advantage to the organism in nature, where sunlight intensity is often the growth-limiting parameter. Successful competition in nature requires capturing more sunlight for self, even if wasted, and preventing light capture by competing neighbors (Melis 2009; Kirst and Melis 2018). Consequently, top layers of plant canopies in agricultural settings, and upper layers of microalgae in high-density liquid cultures absorb direct sunlight far in excess of what is needed to saturate photosynthesis (Nakajima and Ueda 1997; Melis et al. 1999; Polle et al. 2003; Melis 2009; Ort et al. 2011; Kirst and Melis 2014). Excess absorbed irradiance is dissipated in an orderly manner by the photosystems via non-photochemical quenching (NPQ) mechanisms, which evolved to protect the photosynthetic apparatus and prevent photosensitized damage and bleaching (Müller et al. 2001; Ruban 2016; Wobbe et al. 2016; Dall'Osto et al. 2017).

In organisms of oxygenic photosynthesis, large arrays of light-harvesting pigment–protein complexes are assembled as peripheral antenna components of photosystem I (PSI) and photosystem II (PSII) (Jansson et al. 1992; Jansson 1994; Masuda et al. 2002). Minimizing, or truncating, the Chl antenna size of the photosystems would limit excess-absorption of sunlight and can, therefore, improve photosynthetic solar energy conversion efficiency and productivity in cultivations with a high-density foliage (Melis 2009; Ort et al. 2011; Kirst et al. 2017). The rationale in crop plants is that individual chloroplasts and photosystems with a smaller Chl antenna size in the upper canopy leaves will have a diminished probability of absorbing sunlight, thereby permitting greater penetration and a more uniform distribution and utilization of irradiance throughout the foliage of the high-density canopy. Such altered optical properties would alleviate over-absorption and wasteful dissipation of sunlight by the upper canopy, permit greater penetration of sunlight in the canopy interior, and enhance photosynthetic productivity of the foliage as a whole. The truncated light-harvesting antenna (TLA) concept, referring to a smaller than wild-type Chl antenna size of the photosystems, has found noteworthy success in the case of high-density cultivation of microalgae (Nakajima and Ueda 1997, 1999; Melis et al. 1999; Polle et al. 2003; Nakajima et al. 2001; Mussgnug et al. 2007) and cyanobacteria (Nakajima and Ueda 1997, 1999; Kirst et al. 2014).

The situation with crop plants is less clear and more work is needed both to demonstrate the utility of the TLA concept and to identify genes that can be applied in this endeavor. In recent work, Kirst et al. (2017) presented evidence to show that decreasing the light-harvesting antenna size of the photosystems in the existing Su/su Chl-deficient mutant of tobacco (Okabe et al. 1977) helps to increase the photosynthetic productivity and plant canopy biomass accumulation under high-density cultivation conditions. However, Slattery et al. (2017) reported that the Y11y11 and y9y9 Chl-deficient TLA-mutants of soybean (Droppa et al. 1988; Ghirardi and Melis 1988), despite a 50% loss in Chl per leaf area, did not exhibit improvements in canopy-level processes relative to the wild type and showed only a small negative effect on biomass accumulation. Slattery et al. (2017) concluded that soybean significantly overinvests in Chl, a notion pursued in more recent publications (Song et al. 2017; Walker et al. 2017).

Nicotiana tabacum (tobacco), as a model plant system, is readily amenable to nuclear and chloroplast transformations and, therefore, suitable as a platform for foliar production of commodity, immunotherapeutic, and biopharmaceutical products. It offers advantages including the possibility to be coppiced multiple times per year (Andrianov et al. 2010). Large-scale agricultural infrastructure for planting, growing, harvesting and handling tobacco leaves is in place. Therefore, tobacco farmers would benefit using it as a commodity crop plant, and also by planting closer together without canopy shading concerns, thus providing more yield per hectare. However, important for the above considerations is the foliar biomass productivity, improvement of which is the focal point of current effort.

In this work, the TLA concept was applied to high-density tobacco cultivations. Photosynthetic antenna engineering of tobacco was achieved upon downregulation in the expression of the *N. tabacum* nuclear-encoded *CpSRP43* gene, which conferred a TLA property to the plants. CpSRP43 was selected as a downregulation target because it is the first of the CpSRP pathway proteins postulated to engage chloroplast-imported light-harvesting apoproteins in the pathway to thylakoid membrane assembly sites (Kirst and Melis 2014, 2018). The work showed significant biomass accumulation improvements in such TLA tobacco canopies over that measured in wild-type counterparts grown under the same ambient conditions. The work also showed feasibility of gene manipulation in higher plants for the engineering of the Chl antenna size, as a tool for the generation of better performing TLA-crop plants.

Materials and methods

Plant material

Nicotiana tabacum, cv NL Madole Dark (tobacco wild type, Berkeley-ALCS2) and the corresponding transformant "*TLA3-CpSRP43* gene downregulation of expression by RNA interference" (TLA3-RNAi) T1 generation were grown in controlled growth chambers in the lab under artificial illumination (Fig. S1) and in the greenhouse under

ambient sunlight conditions. Plants in the greenhouse were watered with Peter's 20-20-20 nutrients (100 ppm) supplemented with YaraLiva $CaNO_3$ CALCINIT 15.5-0-0 (also 100 ppm), twice per week.

Generation of *TLA3*-RNAi constructs and transformants

Nicotiana tabacum contains two nuclear-encoded *Signal Recognition Particle 43* genes, henceforth referred to as *TLA3* genes (Kirst et al. 2012b), the proteins of which are targeted to the chloroplast (TLA3-CpSRP43). Nucleotide sequence identity between the two *TLA3 CpSRP43* genes found in the genome of *N. tabacum* is greater than 95% (Supplementary Materials). Therefore, efforts to knockdown expression of both genes required the use of only one of the cDNAs, which was cloned into the RNAi vector (Fig. S2). The full length *N. tabacum TLA3 CpSRP43* cDNA (Supplementary Materials) was used to generate the *TLA3-RNAi* transformants (Fig. 1). The pTLA3-RNAi vector was constructed using the pCambia 2300 plasmid as a backbone. HindIII and EcoRI restriction sites were used to clone a CaMV 35S promoter (single enhancer version), a new multiple cloning site, and the RBCS terminator into the backbone. The *Xba*I and *Bam*HI sites of the new multiple cloning site were used to clone intron 11 of the *TLA2 CpFtsY* gene (Kirst et al. 2012a) into the plasmid, splitting the multiple cloning site into two parts to allow the cloning of the forward and reverse direction of the gene. This *TLA2 CpFtsY* gene intron functioned as a spacer between the two directions of the *TLA3 CpSRP43* gene (Fig. 1). The forward and reverse directions of the *TLA3* gene were then cloned into the plasmid leaving minimal cloning scars (see plasmid nucleotide sequence in the Supplementary Materials).

Semi-quantitative reverse transcription-polymerase chain reaction (QRT-PCR)

Total RNA was isolated from tobacco leaves using a Trizol reagent. First-strand cDNA synthesis from both the *TLA3-CpSRP43* and actin transcripts was performed using the Superscript II protocol according to the manufacturer's instructions. QRT-PCR was implemented to evaluate the level of *TLA3-CpSRP43* and actin mRNA using a Biorad S1000 Thermal cycler. The 50-µl PCR reaction mixture included 2.5 units of Taq DNA Polymerase (Qiagen), 1× of 10× PCR buffer, 1 µg of cDNA template, 200 µM of dNTP mix and 0.5 µM of each primer. QRT-PCR was carried out in duplicates to ensure reproducibility of the results. Reaction mixtures were initially heated for 3 min at 94 °C followed by 35 cycles for 1 min at 94 °C, 1 min at 58 °C (TLA3-RNAi)/56 °C (actin), 1 min at 72 °C, and a final 10 min extension at 72 °C for both TLA3-RNAi and actin. Product amplification was determined to be in the linear region of the response at 35 cycles. The PCR products were resolved in an agarose gel (1%) containing GreenGlo Safe DNA Dye (Denville Scientific Inc, Metuchen, NJ, USA). The TLA3-RNAi transcripts expression levels were quantified relative to those of the wild type, normalized to the expression of actin as the reference gene (GenBank accession number: GQ339768). Primers used in this analysis included forward: 5′-ATGGATGCTCTCTTCGTCAA-3′ and reverse: 5′-AGG CGTTTGATTCAAAATCATCC-3′ for the *TLA3-CpSRP43* and forward: 5′-CCATTCTTCGTTTGGACCTT-3′ and reverse: 5′-TTCTGGGCAACGGAACCT-3′ for actin.

Pigment determination and protein analysis

Leaves from wild-type and TLA3-RNAi T1 generation plants were harvested from the middle (partially shaded) and upper (sun-exposed) portion of each of the tobacco canopies. Three independent measurements were conducted with leaf disks from these leaf samples. This was repeated as a function of time during plant growth with samples from three different plants. The Chl concentration and composition of tobacco leaf disks was determined spectrophotometrically from the absorbance of the 100% methanol extracts (Lichtenthaler 1987).

Leaf proteins were extracted upon grinding frozen leaf samples in phosphate-buffered saline and quantified by the Bradford assay. SDS-PAGE (Laemmli 1970) and western blot analyses were conducted for the quantification of the TLA3-CpSRP43 protein level in wild type and TLA3-RNAi transformants. Protein extracts were first resolved in precast TGX-AnyKD SDS-PAGE gels (Bio-Rad), then upon transfer of the resolved proteins to PVDF membranes for

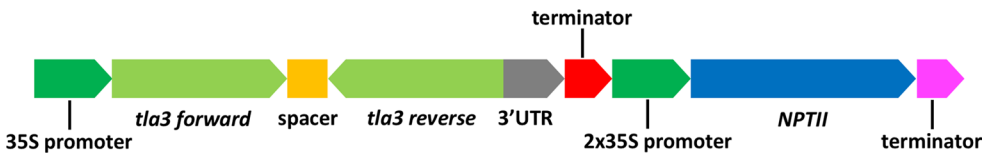

Fig. 1 Schematic presentation of pTLA3-RNAi plasmid for the downregulation of expression of the *TLA3* (*CpSRP43*) gene in *Nicotiana tabacum*. 35S promoter of CaMV; kanamycin-resistant cassette (*NPTII*); *tla3* forward and *tla3* reverse cDNA sequences. The detailed nucleotide descriptions are given in the Supplemental Materials

immuno-detection. Specific polyclonal antibodies for the TLA3-CpSRP43 analysis were raised against the tobacco CpSRP43 oligopeptides KRGKGENVEYLVKWKDGEDN and RTALLFVSGLGSEPCVKLLAEA (Fig. S3; Supplementary Materials). Homemade Tris–glycine-buffered gels, with the running gel solution containing 12% acrylamide–bisacrylamide and 2 M urea, were used to separate denatured polypeptides with a higher resolution than commercial gels. For comparison purposes, loading of samples was done on a per Chl basis.

Native Deriphat-PAGE analysis was done with isolated thylakoid membranes from the wild-type and TLA3-RNAi tobacco. Thylakoids were solubilized at a Chl concentration of 0.5 mg ml^{-1} with *n*-dodecyl-α-D-maltoside (final concentration 1%) by vortexing for 1 min, incubated on ice for 10 min and centrifuged at 20,000*g* for 10 min to remove unsolubilized material. Thylakoid membrane proteins (22 µg Chl per lane) were separated by gradient Deriphat-PAGE; the running gel had an acrylamide concentration gradient from 3.5 to 10.5% (w/v) (29:1 acrylamide–bisacrylamide) containing 12 mM Tris–HCl pH 8.5, 48 mM glycine, and a glycerol gradient from 15 to 25% (w/v). The stacking gel had 3.5% (w/v) acrylamide, 12 mM Tris–HCl pH 8.5, 48 mM, glycine, and 10% (w/v) glycerol. The electrophoresis anode buffer was 12 mM Tris–HCl, pH 8.3, 96 mM glycine. The cathode buffer had the same components as the anode buffer except for the addition of 0.1% (w/v) Deripat-160 (Cognis). The gel was electrophoresed at 50 V constant voltage overnight.

Chloroplast and thylakoid membrane isolation

Leaves from wild-type and TLA3-RNAi T1 generation plants were homogenized in a glass blender in ice-cold chloroplast isolation buffer containing 0.4 M sucrose, 50 mM Tricine (pH 7.8), 10 mM NaCl, 5 mM $MgCl_2$, 0.2% polyvinylpyrrolidone 40, 1% sodium ascorbate, 1 mM aminocaproic acid, 1 mM aminobenzamidine and 100 µM phenylmethylsulfonyl fluoride (PMSF). All operations were conducted at 0 °C with pre-chilled solutions and associated materials. The crude homogenized suspension was filtered through four layers of cheesecloth to remove unbroken leaf pieces and other sizable debris (leaf veins) from the cell lysate. The latter was centrifuged at 5000*g* for 10 min to pellet intact chloroplasts. This soft pellet was gently re-suspended in chilled chloroplast isolation buffer. For thylakoid membrane isolation, chloroplasts were lysed upon re-suspension in hypotonic buffer containing 50 mM Tricine (pH 7.8), 10 mM NaCl, 5 mM $MgCl_2$, 0.2% polyvinylpyrrolidone 40, 1% sodium ascorbate, 1 mM aminocaproic acid, 1 mM aminobenzamidine and 100 µM phenylmethylsulfonyl fluoride followed by passing the suspension through a tight-fitting glass homogenizer. Thylakoid membranes were then pelleted by centrifugation at 75,000*g* for 45 min at 4 °C. Membranes were re-suspended in 50 mM Tricine (pH 7.8), 10 mM NaCl, 5 mM $MgCl_2$ for spectrophotometric analyses.

Spectrophotometric and kinetic analyses

The thylakoid membrane light-minus-dark absorbance difference signal at 700 nm (P700) for PSI (Hiyama and Ke 1972) and 320 nm (Q_A) for PSII (van Gorkom 1974) were measured with a laboratory constructed sensitive absorbance difference spectrophotometer (Melis and Brown 1980; Melis 1989). For P700 quantification measurements, a P700 extinction coefficient of 64 mM^{-1} cm^{-1} was used (Hiyama and Ke 1972).

The functional light-harvesting Chl antenna size of PSI and PSII was estimated from the first-order rate constants of P700 photooxidation and Q_A photo-reduction, measured upon weak green actinic illumination of isolated thylakoid membranes (Melis 1989, 1990). For the functional PSII Chl antenna size, thylakoids were suspended in the presence of 10 µM 3-(3,4-dichlorophenyl)-1,1-dimethylurea (DCMU), thereby blocking electron transport from Q_A to Q_B and the plastoquinone pool. For the functional PSI Chl antenna size, thylakoid membranes were suspended in the presence of DCMU, 200 µM potassium ferricyanide, and 100 µM methyl viologen. The presence of ferricyanide ensured oxidation of the electron carriers between the two photosystems (e.g. the Rieske Fe–S center, cytochrome *f*, and plastocyanin), whereas methyl viologen acted as an efficient electron acceptor from the reducing side of PSI. Such conditions helped to ensure a single photoconversion event in each photosystem, the rate of which was directly proportional to the Chl antenna size. This spectrophotometric kinetic method provided precise measurements of the in situ Chl antenna size of the photosystems from different samples (Melis 1991).

Rate of photosynthesis measurements

Light-saturation curves of photosynthesis were measured by recording the rate of oxygen evolution of leaf disks from three young fully-expanded leaves from three different plants of wild type and TLA3-RNAi, using a LD2/3 Electrode Chamber (Hansatech Instruments, King's Lynn, UK). The starting actinic light intensity was 0 µmol photons m^{-2} s^{-1}, and then increased stepwise to 2.25, 6.5, 17, 38, 60, 150, 175, 310, 470, 570, 800, 1250 and 1450 µmol photons m^{-2} s^{-1}. Measurements of the rate of O_2 evolution/uptake at various light intensities were recorded after the rate of photosynthesis reached a steady state, i.e., after about 5–10 min for light intensities of 570 µmol photons m^{-2} s^{-1} and lower and 2–5 min for light-intensities 800 µmol photons m^{-2} s^{-1} and higher. The method

of asymptotic approximation was used in the estimation of the P_{max} for the TLA3-RNAi samples.

High-density canopy biomass accumulation measurements

High-density canopy biomass accumulation measurements were conducted during the 2016 and 2017 growing seasons, as recently described (Kirst et al. 2017). Wild-type and T1 generation TLA3-RNAi *N. tabacum* seeds were sprinkled on soil in seed pots in the greenhouse nursery for germination. Individual seedlings were transferred to 4 × 4 in. peat pots (Sunshine Mix#1, Sun Gro Horticulture, McClellan Park, CA, USA) for primary growth as individual plants. Growth in the peat pots lasted 2–3 weeks. Following this initial growth, wild-type and TLA3-RNAi plants were transferred into two-gallon pots with a 9-in. diameter. These pots were placed adjacent to and in direct contact with each other to form a tight 5 × 5 canopy configuration of either wild-type or TLA3-RNAi plants, each canopy comprising a 1.3 m^2 (2025 $in.^2$) surface area. Growth and development of the two canopies took place during the same period of time, in the same greenhouse, and under identical ambient and watering conditions. This side-by-side comparison ensured that plants of the two canopies were exposed to identical conditions. A total of six different pairs of wild type and TLA3-RNAi were assessed in this way. Plants in such high-density canopies were allowed to grow for 5–6 weeks, upon which the entire above-ground biomass (25 wild-type and 25 TLA3-RNAi plants) was harvested. A distinction was made between plants growing in the periphery of the canopy (16-plants per canopy), versus those growing in the canopy interior (9-plants per canopy). Moreover, a distinction was made between stem and leaf biomass, which were recorded separately. Fresh weight was recorded immediately after harvesting.

Wild-type and TLA3-RNAi leaf transmittance of solar irradiance was measured with a LI-COR Model LI-185B Quantum/Radiometer/Photometer apparatus equipped with a Quantum photosynthetic active radiation (PAR) sensor.

Statistical analysis of biomass accumulation measurements

A two-tailed paired statistical analysis was used to determine the statistical significance of biomass changes between the TLA3-RNAi and wild-type strains. To avoid pitfalls because of variation in light-intensity or temperature, which would affect biomass accumulation, this analysis was done between individual wild-type and TLA3-RNAi canopy pairs. The following formula was used to calculate the Student *t* test value:

$$t = \frac{\sum D/N}{\sqrt{\frac{\sum D^2 - \left((\sum D)^2/N\right)}{(N-1)\times N}}}$$

where D is the difference between a TLA3-RNAi and wild-type pair and N the number of such pairs. The p value was then calculated using the Student t test.

Results

Screening of the TLA3-RNAi transformant plants

The aim of this TLA3-RNAi knockdown effort was to generate plants with a smaller than wild-type light-harvesting antenna size. However, the efficiency of the *CpSRP43* gene downregulation of expression varied among independent RNAi transformants. Thus, not all transformants showed the same smaller antenna size phenotype. In response, we generated the relatively large number of 34 independent TLA3-RNAi transformants 27 of which were planted in soil and allowed to grow to maturity. We carefully screened all these transformants, initially by measuring the Chl content and composition of the plants to obtain an estimate of the efficiency of the TLA3-RNAi transformation. This approach was based on earlier work, which showed a direct correlation between the expression level of the *TLA3-CpSRP43* gene, the Chl *a*/Chl *b* ratio, and the Chl antenna size of the mutant strains (Kirst et al. 2012a). We selected six of the most promising transformants (T0 lines 7, 9, 12, 17, 21 and 31) to generate self-fertilized T_1 seeds. The T_1 generation segregated into dark green and lighter green plants with a ratio of about 1:3 (Fig. S1). This distribution suggested that heterozygous and homozygous mutant plants have the same lighter green phenotype. Descendants of the three most promising T1 transformants were selected to grow to the T2 seed stage to enable testing for homozygous and heterozygous plants.

Growth and pigmentation characteristics of wild-type (WT) and the TLA3-RNAi tobacco

Coloration differences between the *N. tabacum* wild-type and TLA3-RNAi plants persisted throughout the canopy growth and development (Fig. 2). Wild-type plants (Fig. 2a, c, e) had a darker-green leaf coloration, compared to that of the TLA3-RNAi plants (Fig. 2b, d, f). In such visual comparison, the TLA3-RNAi canopies appeared having a higher density foliage, a qualitative trait supported by detailed biomass quantification measurements (please see below).

Fig. 2 Visual appearance of a pair of *Nicotiana tabacum* wild-type and TLA3-RNAi T1 canopies photographed at different stages of plant development and growth. Wild-type canopies (left-side panels) and TLA3-RNAi canopies (right-side panels) were arranged in a 5 × 5 pot configuration with a 9-in. distance between individual plants. **a**, **b** Small tobacco plants 1 week after transfer from the nursery to the greenhouse and assembly of the 5 × 5 canopy configuration. **c**, **d** Canopies forming at about 3 weeks after setting pots and plants in the greenhouse under ambient conditions. **e**, **f** Dense canopies after 5 weeks of cultivation in the greenhouse. Leaves of the wild type tobacco plants (**a**, **c**, **e**) had a dark green coloration, while leaves of the TLA3-RNAi canopy had a lighter green coloration (**b, d, f**). The wild-type plants also had slightly longer internode distances, as compared to that of the TLA3-RNAi plants. The overall foliage amount at harvest was greater in the TLA3-RNAi canopy, compared to that of the wild type

Earlier work suggested that TLA tobacco may attain a greater leaf thickness compared to that of the wild type (Fig. 1, lower panel in Kirst et al. 2017). This proved to be the case also for the TLA3-RNAi transformants. A measure of this effect was provided from the systematic comparison of leaf dry weight of wild type (1854 µg cm^{-2}) versus that of the TLA3-RNAi (1992 µg cm^{-2}). This analysis showed a gain by about + 7.4% in dry leaf weight for the TLA3-RNAi compared to the wild type (Table 1). Protein content levels were also positively affected in the leaves of the TLA3-RNAi transformants. Wild-type leaves contained on average 341 versus 388 µg protein cm^{-2} measured in TLA3-RNAi leaves. The protein measurements showed a gain by about + 13.8% in the TLA3-RNAi transformants compared to the wild type (Table 1). Chlorophyll content and composition of the leaves in wild-type (WT) and TLA3-RNAi leaves was measured over an extended period of plant growth, as a function of time after planting in the two-gallon 9-in. diameter pots. In all cases and plant developmental stages examined, leaves of the wild type contained more Chl per surface area that those of the TLA3-RNAi (Fig. 3a). Conversely, the Chl *a*/Chl *b* ratio of the TLA3-RNAi leaves was consistently greater (in the vicinity of 5:1), when compared to those of the wild type (about 3.5:1) and independent of the time-after-planting this was assayed (1–60 days after planting). These results showed that the TLA phenotype of the TLA3-RNAi transformants is stable and independent of the plant growth and developmental status.

Chlorophyll content values at the time of canopy harvest for wild type and TLA3-RNAi are shown in Table 1. These pertain to the samples used for the various biochemical measurements conducted in this work. TLA3-RNAi canopy leaves had a lower Chl (*a* and *b*) content, by about − 33.2%, compared to the wild type (Table 1). Among the individual pigments, proportionally more Chl

Table 1 Tobacco wild-type and TLA3-RNAi (T1) canopies were grown in the greenhouse side-by-side

Parameter measured	Wild type	TLA3-RNAi	Difference, %
Leaf dry weight, μg cm^{-2}	1854 ± 58	1992 ± 67	+ 7.4
Protein content, μg cm^{-2}	341 ± 24	388 ± 39	+ 13.8
Chlorophyll (*a* and *b*) content, μg cm^{-2}	38.2 ± 2.7	25.5 ± 3.9	− 33.2
Chlorophyll *a* content, μg cm^{-2}	29.4 ± 1.7	21.3 ± 2.9	− 27.6
Chlorophyll *b* content, μg cm^{-2}	8.7 ± 0.8	4.3 ± 0.55	− 50.6
Chl *a*/Chl *b* ratio, mol:mol	3.45 ± 0.21	5.05 ± 0.24	+ 46.4
Sunlight transmittance through expanded leaves, % of incident irradiance	7.2 ± 1.1	10.7 ± 0.9	+ 48.6
Chl/P700 (mol:mol)	560 ± 10	340 ± 17	− 39.3
Photosystem-II functional antenna size, # of Chl molecules	215 ± 5	146 ± 36	− 32.1
Photosystem-I functional antenna size, # of Chl molecules	195 ± 10	148 ± 4	− 24.1

Leaf Chl content and composition (Chl α and *b*, total Chl, Chl per cm^2 leaf area, Chl *a*/Chl *b* ratio) were measured at the time of harvest. Pigments were extracted from leaf segments in methanol. ± Standard deviation of the mean from six separate sets of wild-type and TLA3-RNAi leaves. Photosystem Chl antenna size measurements were conducted, as previously described (Melis and Thielen 1980; Thielen and van Gorkom 1981; Melis 1989; Kirst et al. 2017)

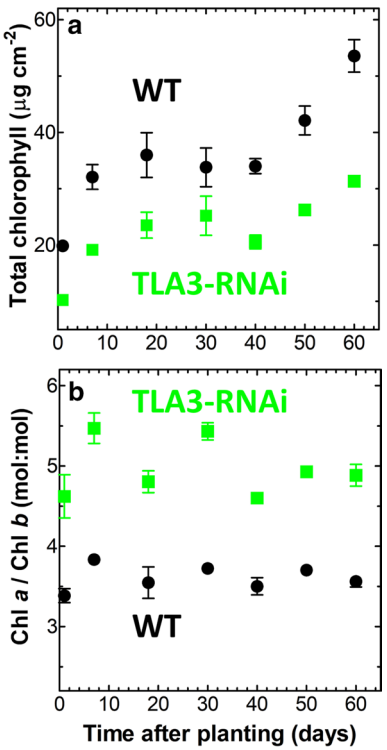

Fig. 3 Chlorophyll content and composition of wild-type (WT) and TLA3-RNAi leaves measured over an extended period of plant growth. Values shown are the average of 6–9 measurements of samples taken from the upper and mid canopies of individual plants. **a** Chlorophyll content per cm^2 leaf surface area of the TLA3-RNAi leaves was consistently lower than that of the wild type throughout the plant development and growth period examined. **b** Chlorophyll *a* to Chl *b* ratios of theTLA3-RNAi leaves was about 5:1, i.e., consistently greater to that of the wild type (3.5:1) throughout the plant development and growth period examined

b was lost (− 50.6%) than Chl *a* (− 27.6%) from the TLA3-RNAi leaves, when compared to the wild type (Table 1). Such uneven changes in Chl *a* and Chl *b* content resulted in a shift of the Chl *a*/Chl *b* ratio from an average value of 3.45:1 in the wild type to 5.05:1 in the TLA3-RNAi leaves. This change in the Chl *a*/Chl *b* ratio suggested the occurrence of a truncated light-harvesting antenna in the photosystems of the TLA3-RNAi transformants, a hypothesis that was investigated in detail (see below).

The different Chl content and composition of wild-type (WT) and TLA3-RNAi leaves impacted sunlight transmittance through the leaves. A measure of this was given by the transmittance of sunlight through fully expanded wild-type (7.2% transmittance of sunlight) versus TLA3-RNAi leaves (10.7% transmittance of sunlight) (Table 1), consistent with the result of recent similar measurements (Kirst et al. 2017).

Downregulation of TLA3-CpSRP43 gene expression by RNAi

To investigate whether the RNAi transformation impacted the expression level of the *TLA3-CpSRP43* gene, we employed QRT-PCR ("Materials and methods") to measure *TLA3-CpSRP43* transcript levels in the wild type and two independent TLA3-RNAi transformant lines (Fig. 4). The highly sensitive QRT-PCR method was chosen because the level of *TLA3-CpSRP43* gene transcripts is low under normal growth conditions, and we anticipated this to be even lower in the transformants. In such QRT-PCR analyses, the actin gene transcripts were chosen to serve as the control. Results in Fig. 4 showed a lower *TLA3-CpSRP43* transcript abundance, down to 45

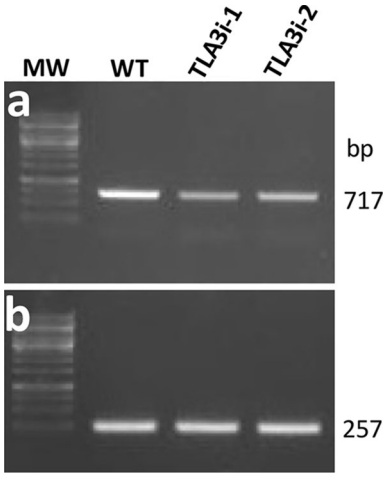

Fig. 4 QRT-PCR analysis of the wild type and two TLA3-RNAi lines probing for the abundance of the mRNA transcripts. **a** Amplification of the *TLA3-CpSRP43* transcripts showing products of 717 bp. Normalized to the wild type (100%), the TLA3i-1 line showed the presence of 45 ± 10% *CpSRP43* transcripts, whereas the TLA3i-2 line had 51 ± 19% transcript abundance. **b** Amplification of the actin gene (GenBank accession number GQ339768) showing equivalent abundance of 257 bp actin transcripts in wild type and TLA3i-1 and TLA3i-2 transformants under these conditions

± 10% in the TLA3i-1 sample and down to 51 ± 19% in the TLA3i-2 sample of the RNAi transformants compared to that of the wild type. It is concluded that the RNAi construct of Fig. 1 brought about a stable downregulation in the level of the TLA3-CpSRP43 transcripts abundance.

Functional light-harvesting Chl antenna size of the photosystems

As hypothesized above, a higher Chl *a*/Chl *b* ratio in the TLA3-RNAi transformants compared to the wild type suggested a Chl-deficiency and a smaller, or truncated, light-harvesting antenna of the photosystems in these transformants. The Chl-deficiency issue was quantified by measuring the ratio of total Chl to P700 (PSI) content in isolated chloroplasts. This ratio measurements showed the presence of 560 Chl molecules per P700 in the wild type and 340 Chl per P700 in the TLA3-RNAi, translating into a −39.3% loss of Chl from the electron-transport chain of the photosynthetic apparatus in the transformants (Table 1).

The functional light-harvesting Chl antenna size of PSI and PSII was measured from the kinetics of P700 photooxidation and Q_A photoreduction, respectively, of isolated thylakoid membranes from the two samples. Methods for this precise in situ determination have been established in the literature (Melis and Thielen 1980; Thielen and van Gorkom 1981; Melis 1989, 1990; Kirst et al. 2017). In the wild type, the average number of the functional PSII Chl antenna size was 215 Chl (*a* and *b*) molecules. This was lowered to about 146 Chl (*a* and *b*) molecules in the TLA3-RNAi transformants, a loss of about −32.1% of the PSII antenna (Table 1). Similarly, the average number of the functional PSI Chl antenna size was 195 Chl (*a* and *b*) molecules. This was lowered to about 148 Chl (*a* and *b*) molecules in the TLA3-RNAi transformants, a loss of about −24.1% of the PSI antenna (Table 1). The results clearly showed the inhibitory effect of the TLA3-RNAi transformation and *N. tabacum CpSRP43* downregulation on the assembly of the peripheral antenna of the photosystems, a result consistent with the *CpSRP43* gene knockout measurements conducted earlier with the green microalga *Chlamydomonas reinhardtii* (Kirst et al. 2012b).

Protein analysis

SDS-PAGE analysis of the leaf constituent proteins was conducted. Wild-type and two independent TLA3-RNAi transformant lines were probed. Loaded on a per Chl basis (2 µg per lane), the SDS-PAGE Coomassie stain showed lower levels of the light-harvesting apoproteins in the TLA3-RNAi transformants than in the wild type (Fig. 5, upper panel marked with arrow). At the same time, there was more Rubisco in the TLA3-RNAi transformant than in the wild type (Fig. 5, upper panel marked with asterisk). Both of these changes are a consequence of the smaller, or truncated, Chl antenna size of the photosystems, so that equal Chl loading results in more Rubisco and less light-harvesting apoprotein in the TLA3-RNAi compared to the wild type.

Western blot analysis of SDS-PAGE-resolved proteins from the wild type and TLA3-RNAi transformants was conducted with specific polyclonal antibodies against the CpSRP43 protein of tobacco (Fig. S3). The results showed a specific cross-reaction of the polyclonal antibodies with the CpSRP43 protein migrating to about 28 kD in these extracts (Fig. 5, lower panel). The amount of the CpSRP43 protein present was somewhat variable in the TLA3-RNAi transformants examined, but always at a level substantially lower than that of the wild type. In the western blot results of Fig. 5 (lower panel), line TLA3-RNAi-1 showed the presence of very low amounts (about 2%) of CpSRP43 present, whereas line TLA3-RNAi-2 had only about 15% of the CpSRP43 protein present, compared to the wild type. Such variations in the efficiency of the RNAi effect are common in the literature, regardless of the species or gene down-regulated. Line TLA3-RNAi-1 was most promising among the transformants down-regulating expression of the CpSRP43 protein. Therefore, it was selected for the more detailed analyses conducted below.

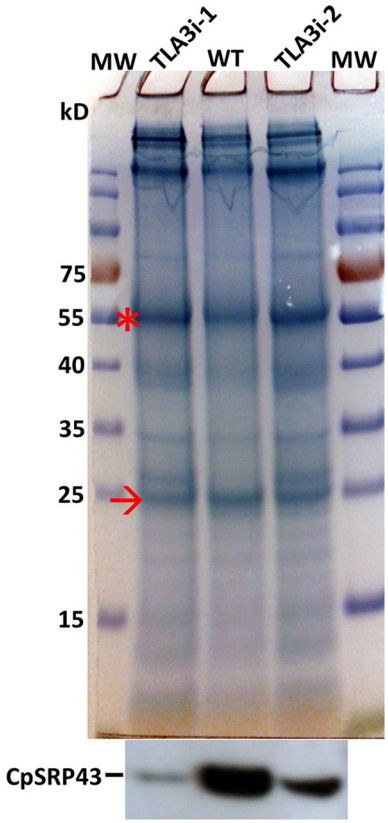

Fig. 5 Upper part SDS-PAGE and Coomassie stain of total leaf protein extracts from *Nicotiana tabacum* wild type (WT) and two TLA3-RNAi T1 lines (TLA3i). Lanes were loaded with 2 µg Chl for the protein analysis. On a Chl basis, the TLA3-RNAi samples contained more RBCL, the large subunit of RubisCO migrating to about 55 kD (marked by red asterisk, *), than the wild type. However, the TLA3-RNAi sample contained lower levels of light-harvesting proteins, migrating in the 25 kD region, reflecting lower apoprotein abundance for the major light-harvesting complex than the wild type (marked by red arrow, →). (The low resolution of the protein bands is due to the presence of excess chlorogenic acid, contained within the tobacco leaves and extracts, which interferes with the SDS-PAGE process.) Lower part western blot analysis of total chloroplast protein extracts from *N. tabacum* wild-type (WT) and TLA3-RNAi leaves. Protein extracts were resolved by SDS-PAGE, transferred onto polyvinylidene difluoride (PVDF) membranes, and probed with specific polyclonal antibodies raised against the TLA3/CpSRP43 protein (please see Supplementary Materials). Note the substantially lower levels of the TLA3/CpSRP43 protein in the TLA3-RNAi samples relative to wild type

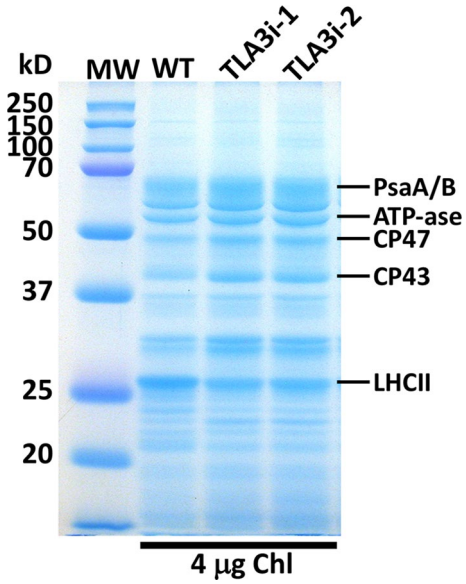

Fig. 6 Denaturing SDS-PAGE and Coomassie stain of proteins from resolved thylakoid membranes isolated from the wild-type and two different TLA3-RNAi tobacco strains. Lanes were loaded with 4 µg Chl. Quantitative differences between wild type and transformants are seen in the amounts of PSI (PsaA/B), CP47/CP43 and LHCII. Relative to the wild type (100%), densitometric scan analysis showed the presence of ~ 124% PsaA/B, 108% ATP-synthase, 142% CP47/CP43, and 66% of LHCII proteins

Light-harvesting apoprotein analysis in wild type and TLA3-RNAi mutants

Isolated thylakoid membranes from wild-type and two different TLA3-RNAi lines were subjected to SDS-PAGE and Coomassie stain analysis (Fig. 6). The results showed that, when loaded on an equal Chl basis, the TLA3-RNAi samples contained more PSII-core CP47 and CP43 apoprotein, but less light-harvesting (LHCII) apoproteins compared with the wild type. These results are consistent with the spectrophotometric and kinetic analysis of antenna size for the two photosystems and show, with a different approach, the TLA properties that were conferred to tobacco upon downregulation in the expression of the *CpSRP43* gene.

An independent assessment of the light-harvesting antenna configuration of wild type and TLA3-TNAi was afforded by green and native blue Deriphat-PAGE analysis with isolated thylakoid membranes from the wild type and TLA3-RNAi tobacco (Fig. 7). The green gel analysis (Fig. 7, left panel) clearly showed a single PSI holocomplex band, comprising the full antenna size of PSI in the wild type, whereas two different TLA3-RNAi lines showed the presence of both the PSI holocomplex and a substantial amount of PSI-core, apparently lacking the corresponding LHCI. In addition, the TLA3-RNAi lines possessed more PSII-core complexes than the wild type, whereas the wild type possessed more LHCII-trimer complexes. A densitometric quantification of these differences is given in the legend in Fig. 7. The corresponding native Coomassie blue Deriphat-PAGE analysis (Fig. 7, right panel) reinforced the breakdown and analysis results shown for the green native gel.

These results are in agreement with the denaturing SDS-PAGE analysis of Fig. 6, and also in agreement with the spectrophotometric and kinetic analysis of antenna size for the two photosystems (Table 1). They further support the

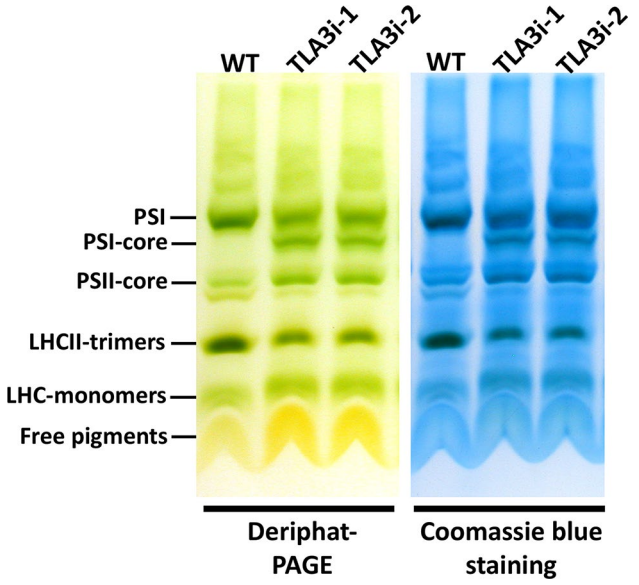

Fig. 7 Analysis of thylakoid membrane protein complexes in the wild-type and TLA3-RNAi mutants by Deriphat-PAGE. *Left panel* green native gel showing the distribution of pigments among the various photosystems and light-harvesting complexes. Quantitative differences between wild type and TLA3-RNAi transformants were seen in the pigment distribution among the PSI, PSII and LHC complexes. Relative to the wild type (100%), densitometric scan analysis of the TLA3-RNAi transformants showed the presence of ~ 115%, PSI (PSI-holocomplex and PSI-core), ~ 200%, PSII-core, ~ 48% LHCII-trimers, and ~ 157% LHC-monomer complexes. *Right panel* the same native Deriphat-PAGE gel stained with Coomassie brilliant blue for the visualization of all constituent protein complexes. Loading of the gels: 22 µg Chl per lane

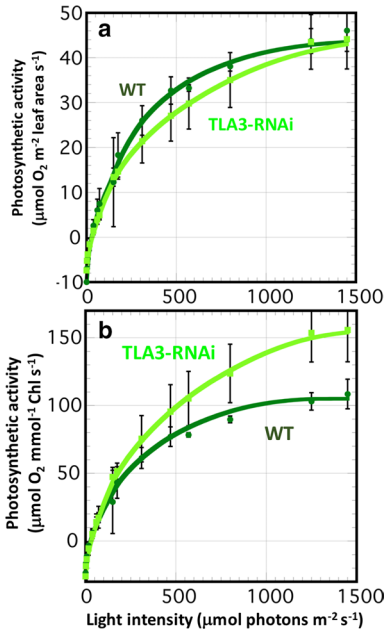

Fig. 8 Light-saturation curves of photosynthesis in *Nicotiana tabacum* wild-type (WT, dark green circles) and TLA3-RNAi leaves (light green squares) at ambient CO_2 concentration (400 µmol mol^{-1}). The half-saturation intensity for the rate of photosynthesis in the wild type was estimated to be 350 ± 5 µmol photons m^{-2} s^{-1}, whereas for the TLA3-RNAi mutant was 450 ± 20 µmol photons m^{-2} s^{-1}. **a** Rates of photosynthesis were measured on a per leaf surface area basis. **b** Rates of photosynthesis were measured on a per leaf Chl content basis

notion of a greater PSII/PSI photosystem ratio in the TLA3-RNAi transformants, compared to that in the wild type, a feature that is commonly encountered in Chl-deficient mutants (Melis 1991).

Light-saturation curves of photosynthesis

To investigate the effect of the TLA3-RNAi transformation on the functional properties of the photosynthetic apparatus in vivo, photosynthesis light-saturation curves were measured for wild-type and transformant leaves. On a per leaf surface area basis (Fig. 8a), the dark respiration rate of wild type and TLA3-RNAi tobacco was about − 9 and − 7 µmol O_2 m^{-2} leaf area s^{-1}, respectively, whereas the light-saturated P_{max} rate was about + 44 and + 47 µmol O_2 m^{-2} leaf area s^{-1} for wild-type and the TLA3-RNAi transformants, respectively. Regardless of the P_{max} rate attained, the photosynthesis half-saturation intensity was about 350 µmol photons m^{-2} s^{-1} for the wild type and 450 µmol photons m^{-2} s^{-1} for the TLA3-RNAi transformants. This difference suggested that photosystems in the TLA3-RNAi tobacco transformants possess only about 70% of the light-harvesting antenna (Chl and Car) compared to that of the wild type. This is consistent with the spectrophotometric and kinetic measurements of the Chl light-harvesting antenna size of the photosystems (Table 1).

A different view of the same type of measurement is offered in the results of Fig. 8b, where photosynthetic activity of the wild type and the TLA3-RNAi tobacco transformant is plotted on a per leaf Chl basis. In this case, the light-saturated P_{max} rate was about + 105 and + 170 µmol O_2 $mmol^{-1}$ Chl s^{-1} for the wild type and TLA3-RNAi transformant, respectively. These P_{max} numbers suggest a substantial increase in the photosynthetic productivity of Chl under light-saturated conditions for the TLA3-RNAi tobacco transformant relative to that of the wild type and played a role at explaining the different biomass productivities among the two different tobacco strains.

Biomass accumulation by individual spatially-separated plants

Wild-type and homozygous T2-generation TLA3-RNAi plants were grown separately and apart from each other in the greenhouse, with a minimum 1 m distance between individual plants to avoid canopy overlap and shading. Plants

were harvested for biomass accumulation measurements at the same time. In such isolated individual cultivations, the TLA-RNAi plants accumulated slightly less (~ 90%) total biomass than the wild type. The slightly lower biomass of the TLA3-RNAi plants could be attributed to the metabolic burden of the kanamycin-resistant cassette, which is constitutively expressed in the transformants and to the resultant minor negative fitness effect this protein may have had on the transformants. The ~ 10% difference in biomass accumulation was consistent. However, it was not statistically significant as evidenced from the Student *t* test, having a *p* value of 0.11 (a value of $p \leq 0.05$ is considered significant).

Biomass accumulation under high canopy and foliage density conditions

Six different 5 × 5 wild-type and TLA3-RNAi tobacco canopy pairs were examined at different times during the growing season, comparing growth and biomass accumulation of the plants in the greenhouse under canopy density conditions. Pairs of wild-type and TLA3-RNAi tobacco canopies (e.g. Fig. 2) were harvested at the same time. The weight of the leaf and stem biomass of the plants was measured separately. Because only the interior nine plants of each canopy were shaded by other plants from all sides, while the periphery 16 plants would have at least one unshaded side, we made a distinction between the interior and periphery canopies. In agronomic configurations covering a large surface area, the interior plants would comprise the majority of the grove and thus the performance of these plants was of particular import in this study.

A pictorial presentation of the percent difference (Δ, %) in total, leaf, and stem biomass accumulation between TLA3-RNAi and the wild type is shown in Figs. 9 and 10

Interior plants of the TLA3-RNAi canopy relative to interior plants of the wild-type canopy showed a + 8.2% increase in total biomass (Fig. 9a). This improvement came about as a result of a + 12.2% gain in leaf biomass and a + 2.7% in stem biomass. Overall, the canopy interior of the TLA3-RNAi transformants showed a + 10% greater leaf/stem ratio, compared to that of the wild type.

Periphery plants of the TLA3-RNAi canopy relative to periphery plants of the wild-type canopy showed a minor change of about + 1.3% in total biomass (Fig. 9b). However, this came about as a result of + 6.2% gain in leaf biomass and a loss of − 6.2% in stem biomass. In consequence, the periphery of the TLA3-RNAi canopy showed a + 14.5% greater leaf/stem ratio compared to that of the wild type.

The total (stem and leaves) average biomass per plant was greater in the TLA3-RNAi (525 g per plant) than wild-type canopies (507 g per plant), a + 3.5% gain (Fig. 10). However, this small gain in the total biomass was not evenly reflected among the leaf and stem biomass. Leaf weight increased

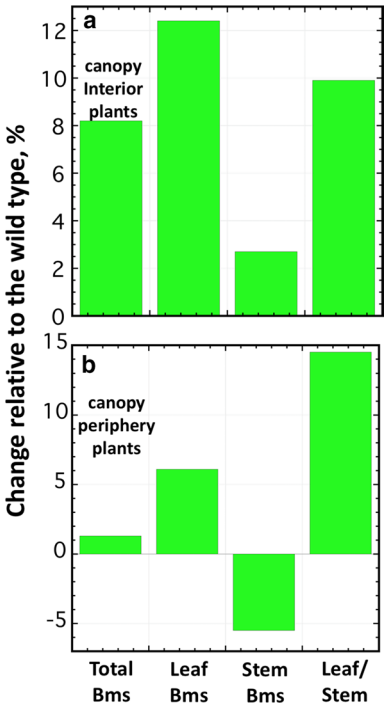

Fig. 9 Distribution of gains and losses between the interior and periphery plants in the 5 × 5 tobacco canopies. **a** TLA3-RNAi plants in the interior of the 5 × 5 canopy accumulated + 8.2% more total biomass than the corresponding wild type. They differentially accumulated + 12.2% more leaf biomass and + 2.7% more stem biomass. TLA3-RNAi plants in the interior of the 5 × 5 canopy showed a + 10% greater leaf/stem ratio than the corresponding wild type. Bms, biomass fresh weight. **b** TLA3-RNAi plants in the periphery of the 5 × 5 canopy accumulated + 1.3% more total biomass than the corresponding wild type. However, this was the result of + 6.2% more leaf biomass and − 6% less stem biomass differential accumulation. These periphery TLA3-RNAi plants showed a + 14.5% greater leaf/stem ratio than the corresponding wild type

from 294 g plant^{-1} in the wild type to 318 g plant^{-1} in the TLA3-RNAi, a + 8.0% gain. Conversely, stem weight decreased from 213 g plant^{-1} in the wild type to 207 g plant^{-1} in the TLA3-RNAi, translating into a − 2.8% loss. As a result of these dissimilar changes, the leaf-to-stem biomass ratio increased from the 1.37:1 in the wild type to 1.54:1 in the TLA3-RNAi transformants, a + 12.7% increase (Fig. 10). These results point to important plant morphology changes emanating from the TLA-property conferred by the TLA3-RNAi downregulation.

Statistical significance of the total, leaf, and stem biomass accumulation

There was qualitative consistency in the patterns described in the results of Figs. 9 and 10 among the six pairs of wild-type and TLA3-RNAi canopy cultivations. However, there were quantitative variations among the six different canopy

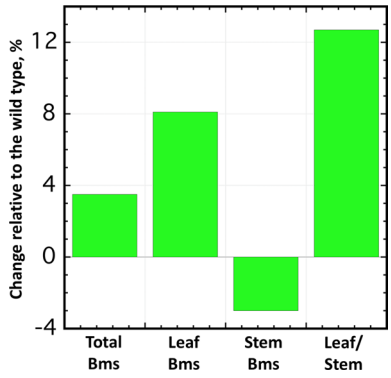

Fig. 10 Harvested biomass difference between the TLA3-RNAi and wild-type tobacco canopies. Values shown are the average from six different pairs of wild-type and TLA3-RNAi canopies grown in the greenhouse (e.g. Fig. 2). TLA3-RNAi canopies produced about 3.5% more total biomass than the wild type. However, this gain was solely attributed to a gain in leaf weight, which exceeded that of the wild type by about 8.1%. TLA3-RNAi canopies produced − 3.2% less stem weight than the wild type. TLA3-RNAi canopies showed a + 12.2% greater leaf-to-stem ratio compared to that of the wild-type canopies. Bms, biomass fresh weight

pairs, as the absolute value of the biomass harvested from each pair differed depending on the time of the year, when the cultivation took place, and the prevailing sunlight conditions, which is variable in the San Francisco Bay Area due to the summer fog. Table 2 shows a detailed canopy-by-canopy analysis of the differences in biomass yield from high-density cultivations of wild type and TLA3-RNAi plants. Stem and leaf biomass were also reported in this canopy-by-canopy analysis. Values shown are the % difference between the TLA3-RNAi and the corresponding wild-type canopies. Table 2 also shows the *p* value that was calculated using a Student *t* test based on all six canopy pairs. Statistically significant Δ values are in bold font. These include whole canopy leaf biomass, peripheral leaf biomass, interior total, and interior leaf biomass. These parameters were significantly greater in the TLA3-RNAi, when compared to those of the corresponding wild-type canopies (Table 2).

Discussion

The TLA concept has been applied, assessed, and discussed rather extensively in microalgae (Nakajima and Ueda 1997, 2000; Melis et al. 1999; Polle et al. 2000, 2003; Nakajima et al. 2001; Mussgnug et al. 2005, 2007; Tetali et al. 2007; Bonente et al. 2011; Kirst et al. 2012a, b; Cazzaniga et al. 2014; Shin et al. 2016; Jeong et al. 2017, 2018) and cyanobacteria (Nakajima and Ueda 1997, 1999; Nakajima and Itayama 2003; Page et al. 2012; Liberton et al. 2013; Lea-Smith et al. 2014; Kirst et al. 2014). The consensus evidence from these measurements is improvement in high-density mass culture productivity at high irradiances, attributed to greater penetration of incident sunlight and more uniform distribution of irradiance in the TLA cultures compared

Table 2 Tobacco wild-type and TLA3-RNAi (T1) biomass yield from high-density cultivations

Parameter measured	Canopy #1Δ, %	Canopy #2Δ, %	Canopy #3Δ, %	Canopy #4Δ, %	Canopy #5Δ, %	Canopy #6Δ, %	Average Δ, %	*p* value
Interior total biomass	8.7	7.2	5.1	1.4	16.7	10.3	**+ 8.2 ± 5.1**	0.012
Interior leaf biomass	10.3	10.1	7.0	5.5	25.3	15.2	**+ 12.2 ± 7.2**	0.011
Interior stem biomass	6.8	3.9	2.7	− 3.6	3.9	2.4	+ 2.7 ± 3.5	0.142
Peripheral total biomass	7.9	− 2.9	− 3.3	8.6	− 1.0	− 1.3	+ 1.3 ± 5.4	0.581
Peripheral leaf biomass	11.3	− 0.2	− 1.3	13.2	6.1	8.0	**+ 6.2 ± 5.9**	0.047
Peripheral stem biomass	3.3	− 6.5	− 6.2	2.7	− 12.5	− 16.9	− 6.0 ± 8.1	0.126
Whole canopy total biomass	8.1	0.2	− 0.7	6.1	4.6	2.4	+ 3.5 ± 3.5	0.065
Whole canopy leaf biomass	11.0	2.9	1.2	10.5	12.0	10.2	**+ 8.1 ± 4.7**	0.009
Whole canopy stem biomass	4.5	− 3.2	− 3.3	0.4	− 7.0	− 10.7	− 3.2 ± 5.3	0.234

Plants were grown in two-gallon pots with the stem-to-stem distance of the plants positioned at 9 in. apart in a 5 × 5 pot configuration. Stem and leaf biomass were measured separately. Values reported are the % difference between the TLA3-RNAi and the corresponding wild-type canopies. ± Standard deviation of the mean from six separate sets of wild-type and TLA3-RNAi canopies. Statistically significant Δ values are bold font

Table 3 Summary of TLA associated genes in green microalgae and cyanobacteria

Strain (*Chlamydomonas reinhardtii*)	Genotype	Antenna size, Chl (*a* + *b*)	Productivity in mass culture (rel. units)	References
Wild type	Normal	430–460	Onefold	Polle et al. (2000, 2003)
tla1	*TLA1*-MOV34/MPN gene downregulation	300	1.5-fold	Polle et al. (2003), Mitra et al. (2012)
tla2	*TLA2*-Δ*CpFTSY* deletion	220	N/A	Kirst et al. (2012a)
tla3	*TLA3*-Δ*CpSRP43* deletion	145	N/A	Kirst et al. (2012b)
tla4	*TLA4*-Δ*CpSRP54* deletion	145	1.6-fold	Jeong et al. (2017)
Lhc-deficient	Δ*Lhc*	N/A	1.8-fold	Mussgnug et al. (2007)
LDT knockout	Δ*CpLtd*	150[a]	1.2-fold	Jeong et al. (2018)
Minimal	Core Chl antenna	130	N/A	Glick and Melis (1988)
Strain (*Synechocystis* PPC 6803)	Genotype	Antenna size, phycobilins and chlorophyll	Productivity in mass culture (rel. units)	References
Wild type	Normal	850	Onefold	Glazer and Melis (1987)
Phycocyanin deficient	Δ*cpc*	520	1.6-fold	Kirst et al. (2014)
Minimal	Core Chl antenna	130	N/A	Glick and Melis (1988)

Known genes and mutations that confer a TLA genotype and the effect of the TLA phenotype on the biomass productivity of the cultures are shown

[a]Denotes a specific adverse effect on the assembly of the Chl antenna size of PSI only

to their wild-type counterparts. Genes that confer a TLA property in microalgae and cyanobacteria have been identified and discussed in the literature (Table 3; Kirst and Melis 2014; Kirst et al. 2017). However, a systematic application of any of these genes to attain a TLA-property in crop plants has not been successfully attempted. This work showed that downregulation of the *TLA3-CpSRP43* gene expression in *N. tabacum* confers the TLA-property to plants and enhances biomass productivity under ambient sunlight in high canopy densities.

A number of crop plants have been identified in the literature as "Chl-deficient" and henceforth shown to possess the TLA-property, including barley (Ghirardi et al. 1986), soybean (Ghiradi and Melis 1988), maize (Greene et al. 1988), sugar beet (Abadia et al. 1985), and tobacco (Thielen and van Gorkom 1981; Kirst et al. 2017). In most of these cases, however, the mutated gene that conferred the TLA property is not yet known. Moreover, until recently, the efficacy of these TLA crop plants for greater photosynthetic productivity under dense cultivation conditions has not been properly assessed. A recent publication from this lab (Kirst et al. 2017) compared the performance of the *N. tabacum*, cv John William's Broadleaf wild type and its Chl-deficient Su/su mutant (Homann and Schmid 1967; Okabe et al. 1977; Thielen and van Gorkom 1981) under conditions of high-density canopy cultivation. The work showed a + 25% greater total biomass accumulation for the TLA tobacco canopies over that measured with their wild-type counterparts, grown under the same ambient conditions. It was suggested that decreasing the light-harvesting antenna size of the photosystems in tobacco, a vascular plant, as the case was for green microalgae and cyanobacteria, helped to increase the photosynthetic productivity and plant canopy biomass accumulation under high-density cultivation conditions (Kirst et al. 2017). However, the gene deletion that resulted in the Okabe et al. (1977) Su/su phenotype has not been identified (but see Fitzmaurice et al. 1999; Hansson et al. 1999 for the role of the tobacco 42 kD Mg-chelatase subunit in Chl-deficiency), making it difficult to potentially apply the Okabe et al. (1977) Su/su property to other crop plants.

The present work applied RNAi-downregulation of the *TLA3-CpSRP43* gene in tobacco, testing for the first time the rational application of molecular genetics in the generation of a TLA-crop plant. The results confirmed the hypothesis that the *CpSRP43* gene is a suitable target for the attainment of TLA crops in which the canopy biomass accumulation under high-density cultivation conditions exceeded that of the corresponding wild type. It should be noted that the benefit of the TLA phenotype was manifested only under high-density canopy conditions. When grown individually and apart from each other, the TLA plants accumulated slightly less biomass then the wild type. The latter was attributed to the metabolic burden of the kanamycin-resistant cassette, which is constitutively expressed in the transformants, and which may comprise metabolic burden affecting fitness.

The work adds to our body of knowledge by showing that an overall greater total biomass accumulation in TLA vs wild-type tobacco canopies is not evenly reflected in the leaf and stem biomass of the plants. The TLA property caused

a substantial increase in the leaf biomass and had a smaller or negative effect on the stem biomass of the plants. It was qualitatively noted earlier (Kirst et al. 2017) that wild-type plants in such canopies tended to have longer internodes compared to TLA plants under similar canopy density conditions. The detailed leaf-to-stem biomass ratios reported in this work helped to substantiate the earlier findings. We hypothesize that enhanced leaf-to-stem biomass ratios in the TLA3-RNAi transformants are an effect of the higher transmittance of sunlight through the TLA3-RNAi canopy leaves, negatively impacting the stem elongation process in the latter. This feature is of interest as it promises to find application and benefit efforts whereby the leaf but not the stem biomass is used for the generation of product, e.g. applications of synthetic biology leading to accumulation of pharmaceuticals, flavors, fragrances, and potentially other useful products. Conversely, a greater leaf-to-stem ratio in TLA compared to wild-type agricultural crop plants may translate into greater seed biomass generated by the former, thereby benefiting world agriculture and enhancing the yield of food generation. Improvements in leaf and overall biomass accumulation reported in this work were likely mitigated by the presence of the transforming vector and the associated antibiotic-resistant cassette in the TLA3-RNAi transformants, which likely exerted a metabolic burden on the cells.

The model plant *N. tabacum* (tobacco) was used in this demonstration. However, the TLA concept could be applied to other crop plants, promising to increase yields, while minimizing the space needed for cultivation. Higher density planting of grapevine, soybean or corn, among other crops, offers additional advantages, as these would achieve canopy closure more quickly, thus causing substantial shading of weed seedlings in the lower canopy (Kirst et al. 2017). In addition, a high-density canopy can significantly minimize losses of soil moisture (Kirst et al. 2017). These advantages can be realized upon the development of grapevine, soybean, corn, among other crop plants, with a truncated light-harvesting Chl antenna size.

Author contribution statement HK, YS, DX, EV, NB and AM designed the project and/or conducted aspects of the experimental work. UW and JAS supported the work and participated in its planning. HK and AM wrote the manuscript. All authors read and edited the manuscript.

Acknowledgements We thank Hannah Clifton and Christina Wistrom for the greenhouse support they provided during the canopy density experiments. We also thank Dr. Peggy G. Lemaux for access to an ESL-1 cabinet and Dr. Krishna K. Niyogi for use of the LD2/3 electrode for oxygen evolution measurements.

Compliance with ethical standards

Conflict of interest The authors declare that they have no conflict of interest.

Human participants and/or animals Research did not involve human and/or animal subjects. Experimental protocols in this work were approved by the UC Berkeley Committee for Laboratory and Environmental BioSafety (CLEB).

Informed consent All authors have read and approved submission of this work.

References

Abadia J, Glick RE, Taylor SE, Terry N, Melis A (1985) Photochemical apparatus organization in the chloroplasts of two *Beta vulgaris* genotypes. Plant Physiol 79:872–878

Andrianov V, Borisjuk N, Pogrebnyak N et al (2010) Tobacco as a production platform for biofuel: overexpression of *Arabidopsis DGAT* and *LEC2* genes increases accumulation and shifts the composition of lipids in green biomass. Plant Biotechnol J 8:277–287

Bonente G, Formighieri C, Mantelli M, Catalanotti C, Giuliano G, Morosinotto T, Bassi R (2011) Mutagenesis and phenotypic selection as a strategy toward domestication of *Chlamydomonas reinhardtii* strains for improved performance in photobioreactors. Photosynth Res 108(2–3):107–120

Cazzaniga S, Dall'Osto L, Szaub J, Scibilia L, Ballottari M, Purton S, Bassi R (2014) Domestication of the green alga *Chlorella sorokiniana*: reduction of antenna size improves light-use efficiency in a photobioreactor. Biotechnol Biofuels 7(1):157

Dall'Osto L, Cazzaniga S, Bressan M, Paleček D, Židek K, Niyogi KK, Fleming GR, Zigmantas D, Bassi R (2017) Two mechanisms for dissipation of excess light in monomeric and trimeric light-harvesting complexes. Nat Plants 3:17033

Droppa M, Ghirardi ML, Horvath G, Melis A (1988) Chlorophyll *b*-deficiency in soybean mutants. II. Thylakoid membrane development and differentiation. Biochim Biophys Acta 932:138–145

Fitzmaurice WP, Nguyen LV, Wernsman EA, Thompson WF, Conkling MA (1999) Transposon tagging of the sulfur gene of tobacco using engineered maize Ac/Ds elements. Genetics 153:1919–1928

Ghirardi ML, Melis A (1988) Chlorophyll *b*-deficiency in soybean mutants. I. Effects on photosystem stoichiometry and chlorophyll antenna size. Biochim Biophys Acta 932:130–137

Ghirardi ML, McCauley SW, Melis A (1986) Photochemical apparatus organization in the thylakoid membrane of *Hordeum vulgare* wild type and chlorophyll *b*-less chlorina *f2* mutant. Biochim Biophys Acta 851:331–339

Glazer AN, Melis A (1987) Photochemical reaction centers: structure, organization, and function. Annu Rev Plant Physiol 38:11–45

Glick RE, Melis A (1988) Minimum photosynthetic unit size in system I and system II of barley chloroplasts. Biochim Biophys Acta 934:151–155

Greene BA, Staehelin LA, Melis A (1988) Compensatory alterations in the photochemical apparatus of a photoregulatory, chlorophyll *b*-deficient mutant of maize. Plant Physiol 87:365–370

Hansson A, Gamini Kannangara C, Von Wettstein D, Hansson M (1999) Molecular basis for semidominance of missense mutations in the XANTHA-H (42-kDa) subunit of magnesium chelatase. Proc Natl Acad Sci USA 96:1744–1749

Hiyama T, Ke B (1972) Difference spectra and extinction coefficients of P 700. Biochim Biophys Acta (BBA) Bioenerg 267:160–171

Homann PH, Schmid GH (1967) Photosynthetic reactions of chloroplasts with unusual structures. Plant Physiol 42:1619–1632
Jansson S (1994) The light-harvesting chlorophyll *a/b*-binding proteins. Biochim Biophys Acta 1184(1):1–19
Jansson S, Pichersky E, Bassi R, Green BR, Ikeuchi M, Melis A, Simpson DJ, Spangfort M, Staehelin LA, Thornber JP (1992) A nomenclature for the genes encoding the chlorophyll *a–b*-binding proteins of higher plants. Plant Mol Biol Rep 10:242–253
Jeong J, Baek K, Kirst H, Melis A, Jin E (2017) Loss of CpSRP54 function leads to a truncated light-harvesting antenna size in *Chlamydomonas reinhardtii*. Biochim Biophys Acta 1858:45–55
Jeong J, Baek K, Jihyeon YuJ, Kirst H, Betterle N, Shin W, Bae S, Melis A, Jin ES (2018) Deletion of the chloroplast LTD protein impedes LHCI import and PSI-LHCI assembly in *Chlamydomonas reinhardtii*. J Exp Bot 69:1147–1158
Kirst H, Melis A (2014) The chloroplast *Signal Recognition Particle* pathway (CpSRP) as a tool to minimize chlorophyll antenna size and maximize photosynthetic productivity. Biotech Adv 32:66–72
Kirst H, Melis A (2018) Improving photosynthetic solar energy conversion efficiency: the truncated light-harvesting antenna (TLA) concept. In: Seibert M, Torzillo G (eds) Microalgal hydrogen production: achievements and perspectives, chap 14. European Society for Photobiology 2018. Royal Society of Chemistry, London, pp 335–353
Kirst H, Garcia-Cerdan JG, Zurbriggen A, Melis A (2012a) Assembly of the light-harvesting chlorophyll antenna in the green alga *Chlamydomonas reinhardtii* requires expression of the *TLA2-CpFTSY* gene. Plant Physiol 158:930–945
Kirst H, Garcia-Cerdan JG, Zurbriggen A, Ruehle T, Melis A (2012b) Truncated photosystem chlorophyll antenna size in the green microalga *Chlamydomonas reinhardtii* upon deletion of the *TLA3-CpSRP43* gene. Plant Physiol 160(4):2251–2260
Kirst H, Formighieri C, Melis A (2014) Maximizing photosynthetic efficiency and culture productivity in cyanobacteria upon minimizing the phycobilisome light-harvesting antenna size. Biochim Biophys Acta Bioenerg 1837:1653–1664
Kirst H, Gabilly ST, Niyogi KK, Lemaux PG, Melis A (2017) Photosynthetic antenna engineering to improve crop yields. Planta 245:1009–1020
Laemmli UK (1970) Cleavage of structural proteins during the assembly of the head of bacteriophage T4. Nature 227:680–685
Lea-Smith DJ, Bombelli P, Dennis JS, Scott SA, Smith AG, Howe CJ (2014) Phycobilisome deficient strains of *Synechocystis* sp PCC6803 have reduced size and require carbon limiting conditions to exhibit enhanced productivity. Plant Physiol 165:705–714
Liberton M, Collins AM, Page LE, O'Dell WO, O'Neill H, Urban WS, Timlin JA, Pakrasi HB (2013) Probing the consequences of antenna modification in cyanobacteria. Photosynth Res 118:17–24
Lichtenthaler HK (1987) Chlorophylls and carotenoids: pigments of photosynthetic biomembranes. Methods Enzymol 148:350–382
Masuda T, Polle JEW, Melis A (2002) Biosynthesis and distribution of chlorophyll among the photosystems during recovery of the green alga *Dunaliella salina* from irradiance stress. Plant Physiol 128:603–614
Melis A (1989) Spectroscopic methods in photosynthesis: photosystem stoichiometry and chlorophyll antenna size. Philos Trans R Soc Lond B 323:397–409
Melis A (1990) Regulation of photosystem stoichiometry in oxygenic photosynthesis. In: Kanai R, Katoh S, Miyachi S (eds) Regulation of photosynthetic processes. Botanical magazine Tokyo, special issue vol 2. University of Tokyo Press, Tokyo, pp 9–28
Melis A (1991) Dynamics of photosynthetic membrane composition and function. Biochim Biophys Acta 1058:87–106
Melis A (2009) Solar energy conversion efficiencies in photosynthesis: minimizing the chlorophyll antennae to maximize efficiency. Plant Sci 177:272–280
Melis A, Brown JS (1980) Stoichiometry of system I and system II reaction centers and of plastoquinone in different photosynthetic membranes. Proc Natl Acad Sci USA 77:4712–4716
Melis A, Thielen APGM (1980) The relative absorption cross-section of photosystem I and photosystem II in chloroplasts from three types of *Nicotiana tabacum*. Biochim Biophys Acta 589:275–286
Melis A, Neidhardt J, Benemann JR (1999) *Dunaliella salina* (Chlorophyta) with small chlorophyll antenna sizes exhibit higher photosynthetic productivities and photon use efficiencies than normally pigmented cells. J Appl Phycol 10:515–525
Mitra M, Ng S, Melis A (2012) The TLA1 protein family members contain a variant of the plain MOV34/MPN domain. Am J Biochem Mol Biol 2(1):1–18
Müller P, Li X-P, Niyogi KK (2001) Non-photochemical quenching: a response to excess light energy. Plant Physiol 125:1558–1566
Mussgnug JH, Wobbe L, Elles I, Claus C, Hamilton M, Fink A, Kahmann U, Kapazoglou A, Mullineaux CW, Hippler M, Nickelsen J, Nixon PJ, Kruse O (2005) NAB1 is an RNA binding protein involved in the light-regulated differential expression of the light-harvesting antenna of *Chlamydomonas reinhardtii*. Plant Cell 17:3409–3421
Mussgnug JH, Thomas-Hall S, Rupprecht J, Foo A, Klassen V, McDowall A, Schenk PM, Kruse O, Hankamer B (2007) Engineering photosynthetic light capture: impacts on improved solar energy to biomass conversion. Plant Biotech J 5:802–814
Nakajima Y, Itayama T (2003) Analysis of photosynthetic productivity of microalgal mass cultures. J Appl Phycol 15:450–497
Nakajima Y, Ueda R (1997) Improvement of photosynthesis in dense microalgal suspension by reduction of light harvesting pigments. J Appl Phycol 9:503–510
Nakajima Y, Ueda R (1999) Improvement of microalgal photosynthetic productivity by reducing the content of light harvesting pigments. J Appl Phycol 11:195–201
Nakajima Y, Ueda R (2000) The effect of reducing light-harvesting pigment on marine microalgal productivity. J Appl Phycol 12(3–5):285–290
Nakajima Y, Tsuzuki M, Ueda R (2001) Improved productivity by reduction of the content of light-harvesting pigment in *Chlamydomonas perigranulata*. J Appl Phycol 13:95–101
Okabe K, Schmid GH, Straub J (1977) Genetic characterization and high efficiency photosynthesis of an aurea mutant of tobacco. Plant Physiol 60:150–156
Ort DR, Zhu XG, Melis A (2011) Optimizing antenna size to maximize photosynthetic efficiency. Plant Physiol 155:79–85
Page LE, Liberton M, Pakrasi H (2012) Reduction of photoautotrophic productivity in the cyanobacterium *Synechocystis* sp strain PCC 6803 by phycobilisome antenna truncation. Appl Environ Microbiol 78:6349–6351
Polle JEW, Benemann JR, Tanaka A, Melis A (2000) Photosynthetic apparatus organization and function in wild type and a Chl *b*-less mutant of *Chlamydomonas reinhardtii.* Dependence on carbon source. Planta 211:335–344
Polle JE, Kanakagiri SD, Melis A (2003) *tla1*, a DNA insertional transformant of the green alga *Chlamydomonas reinhardtii* with a truncated light-harvesting chlorophyll antenna size. Planta 217:49–59
Ruban AV (2016) Non-photochemical chlorophyll fluorescence quenching: mechanism and effectiveness in protection against photodamage. Plant Physiol 170:1903–1916
Shin WS, Lee BR, Chang YK, Kwon JH (2016) Truncated light-harvesting chlorophyll antenna size in *Chlorella vulgaris* improves biomass productivity. J Appl Phycol 28:3193–3202

Slattery RA, VanLoocke A, Bernacchi CJ, Zhu XG, Ort DR (2017) Photosynthesis, light use efficiency, and yield of reduced-chlorophyll soybean mutants in field conditions. Front Plant Sci 8:549

Song Q, Wang Y, Qu M, Ort DR, Zhu XG (2017) The impact of modifying photosystem antenna size on canopy photosynthetic efficiency-development of a new canopy photosynthesis model scaling from metabolism to canopy level processes. Plant Cell Environ 40:2946–2957

Tetali SD, Mitra M, Melis A (2007) Development of the light-harvesting chlorophyll antenna in the green alga *Chlamydomonas reinhardtii* is regulated by the novel *Tla1* gene. Planta 225:813–829

Thielen APGM, Van Gorkom HL (1981) Quantum efficiency and antenna size of photosystem II-alpha, II-beta and I in tobacco chloroplasts. Biochim Biophys Acta 635:111–120

Van Gorkom HJ (1974) Identification of the reduced primary electron acceptor of photosystem II as a bound semiquinone anion. Biochim Biophys Acta 347:439–442

Walker BJ, Drewry DT, Slattery RA, VanLoocke A, Cho YB, Ort DR (2017) Chlorophyll can be reduced in crop canopies with little penalty to photosynthesis. Plant Physiol. https://doi.org/10.1104/pp.17.01401

Wobbe L, Bassi R, Kruse O (2016) Multi-level light capture control in plants and green algae. Trends Plant Sci 21(1):55–68